Large Decay of X-ray Flux in 2XMM J123103.2+110648: Evidence for a Tidal Disruption Event

Dacheng Lin – University of New Hampshire
Olivier Godet – Université de Toulouse
Luis C. Ho – Peking University
Didier Barret – Université de Toulouse
Natalie A. Webb – Université de Toulouse
Jimmy A. Irwin – University of Alabama

Citation of published version:

Lin, D., Godet, O., Ho, L., Barret, D., Webb, N., Irwin, J. (2017): Large Decay of X-ray Flux in 2XMM J123103.2+110648: Evidence for a Tidal Disruption Event. *Monthly Notices of the Royal Astronomical Society*, 468 (1). DOI: 10.1093/mnras/stx489

Monthly Notices
of the
ROYAL ASTRONOMICAL SOCIETY

MNRAS **468,** 783–789 (2017)
Advance Access publication 2017 February 24
doi:10.1093/mnras/stx489

Large decay of X-ray flux in 2XMM J123103.2+110648: evidence for a tidal disruption event

Dacheng Lin,[1★] Olivier Godet,[2,3] Luis C. Ho,[4,5] Didier Barret,[2,3] Natalie A. Webb[2,3] and Jimmy A. Irwin[6]

[1] *Space Science Center, University of New Hampshire, Durham, NH 03824, USA*
[2] *CNRS, IRAP, 9 avenue du Colonel Roche, BP 44346, F-31028 Toulouse Cedex 4, France*
[3] *Université de Toulouse, UPS-OMP, IRAP, F-31028 Toulouse, France*
[4] *Kavli Institute for Astronomy and Astrophysics, Peking University, Beijing 100871, China*
[5] *Department of Astronomy, School of Physics, Peking University, Beijing 100871, China*
[6] *University of Alabama, Department of Physics and Astronomy, Tuscaloosa AL 35487, USA*

Accepted 2017 February 22. Received 2017 February 17; in original form 2016 December 9

ABSTRACT

The X-ray source 2XMM J123103.2+110648 was previously found to show pure thermal X-ray spectra and an ∼3.8 h periodicity in three *XMM–Newton* X-ray observations in 2003–2005, and the optical spectrum of the host galaxy suggested it as a type 2 active galactic nucleus candidate. We have obtained new X-ray observations of the source, with *Swift* and *Chandra* in 2013–2016, in order to shed new light on its nature based on its long-term evolution property. We found that the source could be in an X-ray outburst, with the X-ray flux decreasing by an order of magnitude in the *Swift* and *Chandra* observations, compared with the *XMM–Newton* observations 10 yr ago. There seemed to be significant spectral softening associated with the drop of X-ray flux (disc temperature $kT \sim 0.16$–0.2 keV in *XMM–Newton* observations versus $kT \sim 0.09 \pm 0.02$ keV in the *Chandra* observation). Therefore, the *Swift* and *Chandra* follow-up observations support our previous suggestion that the source could be a tidal disruption event (TDE), though it seems to evolve slower than most of the other TDE candidates. The apparent long duration of this event could be due to the presence of a long super-Eddington accretion phase and/or slow circularization.

Key words: accretion, accretion discs – black hole physics – galaxies: individual: 2XMM J123103.2+110648 – X-rays: galaxies.

1 INTRODUCTION

Active galactic nuclei (AGN) typically show hard X-ray spectra (photon index ∼2.0 when 2–10 keV spectra are fitted with an absorbed power-law), in addition to a possible soft excess below around 1.0 keV (Wilkes & Elvis 1987; Turner & Pounds 1989; Comastri et al. 1992; Nandra & Pounds 1994; Gierliński & Done 2004; Lin, Webb & Barret 2012). Very few galactic nuclei exhibit pure thermal X-ray spectra with the hard X-ray component either extremely weak or completely absent. Most of these outliers are observed in the candidate tidal disruption events (TDEs), in which stars are tidally disrupted and subsequently accreted by massive black holes (BHs) at the centre of galaxies (for recent reviews, refer to Komossa 2012, 2015). About 30 such TDEs have been found, with host galaxies showing no sign or weak sign of persistent nuclear activity in the optical spectra. However, pure thermal X-ray spectra were also detected in several galactic nuclei with clear narrow emission lines in optical, suggesting possible persistent nuclear activity. Good examples of such objects include GSN 069 (Miniutti et al. 2013), 2XMM J123103.2+110648 (hereafter, XJ1231+1106 ; Ho et al. 2012; Lin et al. 2012; Terashima et al. 2012; Lin et al. 2013a; Lin, Webb & Barret 2014) and IC 3599 (Grupe et al. 1995; Campana et al. 2015; Grupe, Komossa & Saxton 2015).

GSN 069 was discovered in 2010 and was found to be in an outburst, with the X-ray flux a factor of >240 higher than *ROSAT* observations in the early 1990s. The outburst seems to be semipersistent, with the flux remaining fairly steady since it was discovered (Miniutti et al. 2013). The X-ray spectra were supersoft, consistent with sub-Eddington thermal disc emission from a BH of mass $\sim 10^6$ $M_\odot$ (Miniutti et al. 2013). The optical spectrum exhibited no broad emission lines but only narrow ones suggesting a low-luminosity Seyfert 2 galaxy.

XJ1231+1106 was serendipitously detected by *XMM–Newton* in two epochs separated by 2.4 yr, with the luminosity slightly

⋆ E-mail: dacheng.lin@unh.edu

lower in the first epoch than in the second one. In the second epoch there were two observations four days apart, with a ∼3.8 h quasi-periodic oscillation significantly (∼5σ) detected in both of them (Lin et al. 2013a). The optical spectrum of its host galaxy SDSS J123103.24+110648.6 (hereafter GJ1231+1106) also exhibited no broad emission lines, but narrow ones consistent with a low-luminosity AGN (Ho et al. 2012). The width of the narrow lines is so small (velocity dispersion $\sigma = 34$ km s^{-1} for [O III] λ5007) that Ho et al. (2012) inferred the BH mass to be only $\sim 10^5$ M$_\odot$.

IC 3599 has at least two outbursts since it was discovered in 1990 (Grupe et al. 1995, 2015; Campana et al. 2015). It had ultrasoft X-ray spectra in the peak of the outbursts, though in the low state it behaved as a typical AGN. The repeated outbursts were explained as recurrent partial disruption of a star by the central supermassive BH (Campana et al. 2015) or as AGN flares caused by a disc instability (Grupe et al. 2015).

In this paper, we continue to study XJ1231+1106. The source evolution on time-scales longer than the *XMM–Newton* observations was unclear. Although it was not detected in the *ROSAT* All-Sky Survey, the non-detection could be just because of the low sensitivity of the survey, which had a detection limit of 5×10^{-13} erg s^{-1} cm^{-2} in 0.1–2.4 keV (Voges et al. 1999), five times higher than the fluxes of the source in the *XMM–Newton* observations. We have obtained *Swift* and *Chandra* follow-up observations of the source and found a significant decrease in the X-ray flux. We report this finding in this paper. Here, we also fit the optical spectrum of the host galaxy GJ1231+1106 taken by the SDSS, aiming to reveal more properties of the environment of XJ1231+1106. In Section 2, we describe the data analysis. In Section 3, we present the results. The discussion of the source nature and our conclusions are given in Section 4.

2 DATA ANALYSIS

2.1 *Swift* observations

At our request, *Swift* (Gehrels et al. 2004) carried out 11 observations of XJ1231+1106 between 2013 March and 2014 July (Table 1). The first two observations had been studied in Lin et al. (2013a), and here we analyse all observations with FTOOLS 6.19 and updated calibration files (released on 2016 November 1). The X-ray telescope (Burrows et al. 2005) was operated in photon counting mode. We reprocessed the event files with the task XRTPIPELINE (version 0.13.2). The source was not clearly detected in any observation. In order to probe a deeper sensitivity, we created a co-added spectrum from all observations (total exposure time 51 ks) using a source region of radius 20 arcsec and a background region of radius 2 arcmin. The UV-Optical Telescope (Roming et al. 2005) used the UVW1 filter (8.3 ks) in the first observation and the UVW2 filter in the other observations (total exposure 41.1 ks). The UV magnitudes and fluxes were measured with the task *uvotsource* with a source region of radius 5 arcsec and a background region of radius 25 arcsec. This is done both for individual observations and for the merged observation (the UVW2 filter).

2.2 *Chandra* observation

We had a follow-up observation of XJ1231+1106 with *Chandra* on 2016 February 10 (Table 1). It used the imaging array of the *AXAF* CCD Imaging Spectrometer (Bautz et al. 1998), with the aim point at the back-illuminated chip S3, given that the source had been ultrasoft. We reprocessed the data with the script *chandra_repro* in the *Chandra* Interactive Analysis of Observations (CIAO, version 4.8) package and applied the latest calibration (CALDB 4.7.2). The exposure time of the observation is 39.5 ks, without background flares. We extracted the source and background spectra and created the corresponding response matrices for all observations using the script *specextract*. The radius of the source region used was 1.6 arcsec, corresponding to point spread function enclosing fractions of 95 per cent at 1.0 keV, and the radius of the background region was 30 arcsec.

Table 1. X-ray observations and spectral fit results[a].

Observation ID	Start date	$kT_{\rm MCD}$ (keV)	$F_{\rm X}$[b] (10^{-13} erg s^{-1} cm^{-2})	$F_{\rm bol}$[c]
XMM–Newton:				
0145800101	2003–07–13	$0.16^{+0.01}_{-0.01}$	$0.65^{+0.11}_{-0.06}$	$1.48^{+0.33}_{-0.20}$
0306630101	2005–12–13	$0.20^{+0.01}_{-0.01}$	$1.38^{+0.18}_{-0.10}$	$2.55^{+0.45}_{-0.24}$
0306630201	2005–12–17	$0.18^{+0.01}_{-0.01}$	$1.04^{+0.15}_{-0.08}$	$2.17^{+0.44}_{-0.23}$
Swift:				
00032732001	2013-03-08	$0.15^{+0.07}_{-0.05}$	$0.16^{+0.09}_{-0.07}$	$0.39^{+0.44}_{-0.20}$
00032732002	2013-06-21			
00032732003	2013-11-21			
00032732004	2014-01-04			
00032732005	2014-01-08			
00032732006	2014-02-13			
00032732007	2014-03-29			
00032732008	2014-05-08			
00032732009	2014-05-13			
00032732010	2014-06-17			
00032732011	2014-07-27			
Chandra:				
17129	2016-02-10	$0.09^{+0.03}_{-0.02}$	$0.09^{+0.05}_{-0.04}$	$0.52^{+0.59}_{-0.29}$

Notes. [a]The fits used the MCD model. All uncertainties are at the 90 per cent confidence level. The fits to *XMM–Newton* observations are from Lin et al. (2013a) and we refer to it for more details.
[b]Unabsorbed 0.34–11 keV (source rest frame) flux.
[c]Unabsorbed bolometric flux (based on the MCD component).

2.3 The SDSS spectroscopic observation

The SDSS took a spectrum of the host galaxy of XJ1231+1106 on 2012 January 23. We fitted the spectrum with multicomponent models comprised of single-population synthetic spectra, using penalized pixel fitting (PPXF) software (Cappellari & Emsellem 2004) and Vazdekis et al. (2010) synthetic spectra spanning a grid of 48 ages between 0.06 to 14 Gyr and seven metallicities [M/H] = $\{-2.32, -1.71, -1.31, -0.71, -0.40, 0.00, +0.22\}$. The spectrum also exhibits narrow emission lines, which were fitted with Gaussian functions. No additive or multiplicative polynomials were included in the fit. The spectrum was corrected for the Galactic dust reddening (Schlegel, Finkbeiner & Davis 1998) of $E(B-V)_{\rm G} = 0.03$ mag before the fit. The intrinsic reddening was left as a free fitting parameter and was inferred to be negligible.

3 RESULTS

3.1 The host galaxy

The SDSS spectrum of the host galaxy GJ1231+1106 is shown in Fig. 1. The PPXF fit of the star component is shown as a red line. The light-weighted age is 5.9 Gyr, and the mass-weighted age is 7.8 Gyr. The total stellar mass is $\sim 5.5 \times 10^9$ M$_\odot$, and the total luminosity within the fitting band (source rest frame 3540–7410 Å)

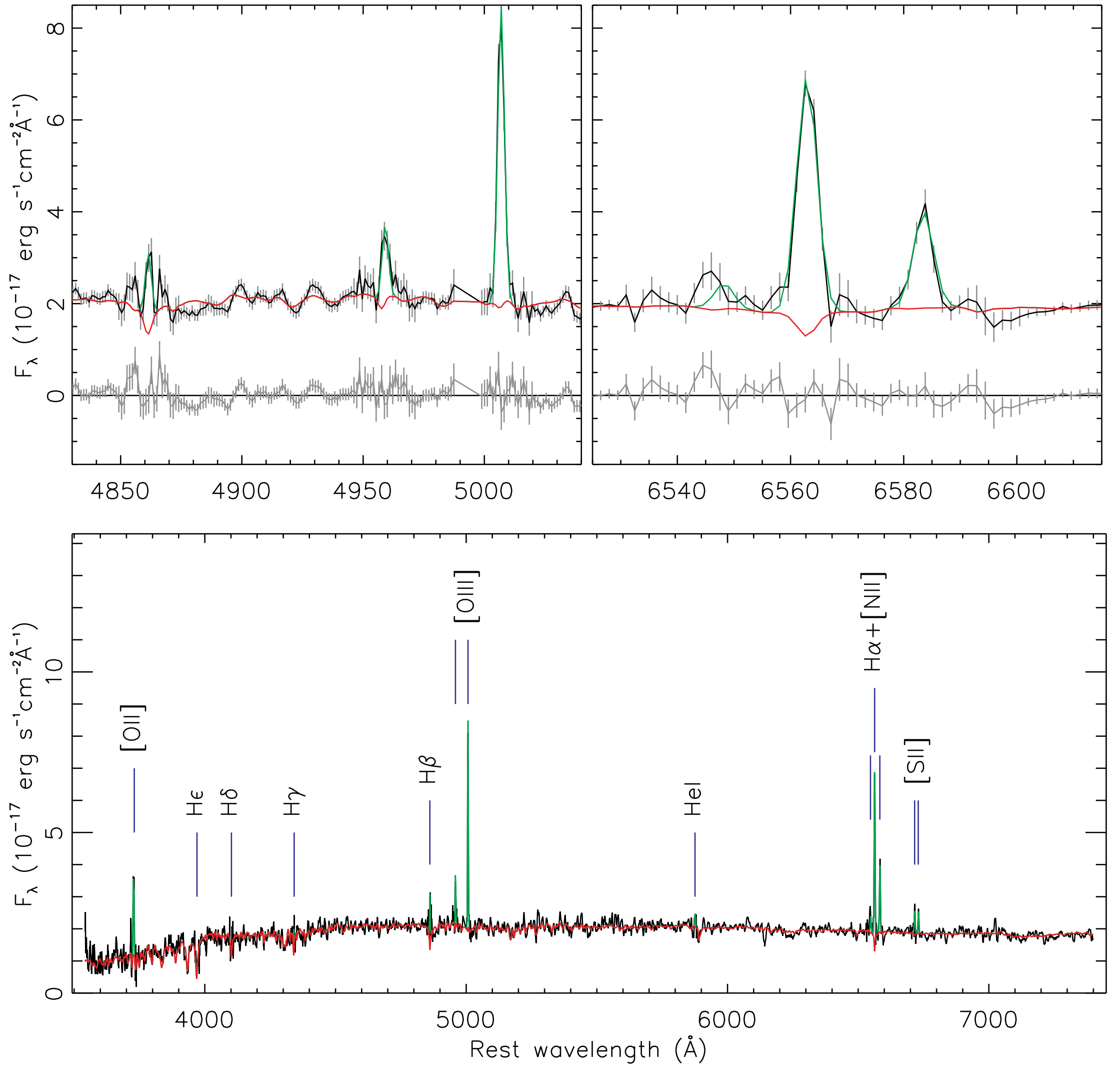

Figure 1. The SDSS optical spectrum of the candidate host galaxy of XJ1231+1106 taken on 2012 March 3, showing only narrow emission lines. The upper two panels zoom into the Hβ-[O III] complex and the Hα-[N II] region, with the fit residuals. The PPXF fit is shown as a solid green line, while the star component is shown as a red line. The data points outside the emission line regions have been smoothed with a box function of width 5 for clarity.

is $\sim 7.8 \times 10^8$ L$_\odot$, indicating a dwarf host galaxy (mass comparable to the Large Magellanic Cloud). Based on the relation between the BH mass and the total galaxy stellar mass from Reines & Volonteri (2015), we estimated that the BH mass to be 1.5×10^6 M$_\odot$ (an intrinsic scatter of 0.55 dex). The mass and light distributions of the stellar populations are shown in Fig. 2. There seems to be a young population of age <90 Myr, suggesting some level of star-forming activity.

The PPXF fit inferred the intrinsic width of the emission lines to be $\sigma = 43 \pm 4$ km s^{-1}. This value is below the SDSS instrumental resolution (70 km s^{-1}) and thus should be taken with caution, though it is consistent with that obtained by Ho et al. (2012), using a Magellan spectrum with a much higher resolution. The intrinsic reddening of the emission lines is $E(B-V)_{\rm i} = 0.29$ mag, assuming an intrinsic Hα/Hβ ratio of 3.1. Accounting for this small intrinsic reddening, the line ratios put the source in the Seyfert region on the BPT diagrams (see Fig. 3; Baldwin, Phillips & Terlevich 1981; Veilleux & Osterbrock 1987), but close to the boundary between the H II and Seyfert regions. This indicates some level of star-forming activity, which is consistent with the fit of the star component, and/or the low metallicity of the host (e.g. Ludwig et al. 2012).

There is a faint UV source from the *Swift* observation at the position of GJ1231+1106. We obtained the W1 magnitude of 22.6 $\pm$ 0.2 AB mag (flux $1.4 \pm 0.2 \times 10^{-17}$ erg s^{-1} cm^{-2} Å^{-1}) in the first *Swift* observation. The mean W2 magnitude is 23.2 ± 0.1 AB mag (flux $1.3 \pm 0.1 \times 10^{-17}$ erg s^{-1} cm^{-2} Å^{-1}) from the merged observation. The ten individual observations gave consistent W2 magnitudes (mostly within 1σ but none above 3σ). Therefore, we did not detect significant variability in the W2 filter. Based on the W1 and W2 photometry, the UV source seems blue and can be explained with the presence of some star-forming activity.

3.2 X-ray Follow-up

In the *Chandra* follow-up observation in 2016, we obtained 13 counts within 0.24–7 keV, with 0.7 background counts, at the position of XJ1231+1106. The net source count rate is $3.1 \pm 0.9 \times 10^{-4}$ counts s^{-1} (1σ uncertainty), a factor of 26 lower than expected from the second *XMM–Newton* spectrum (obtained on 2005 December

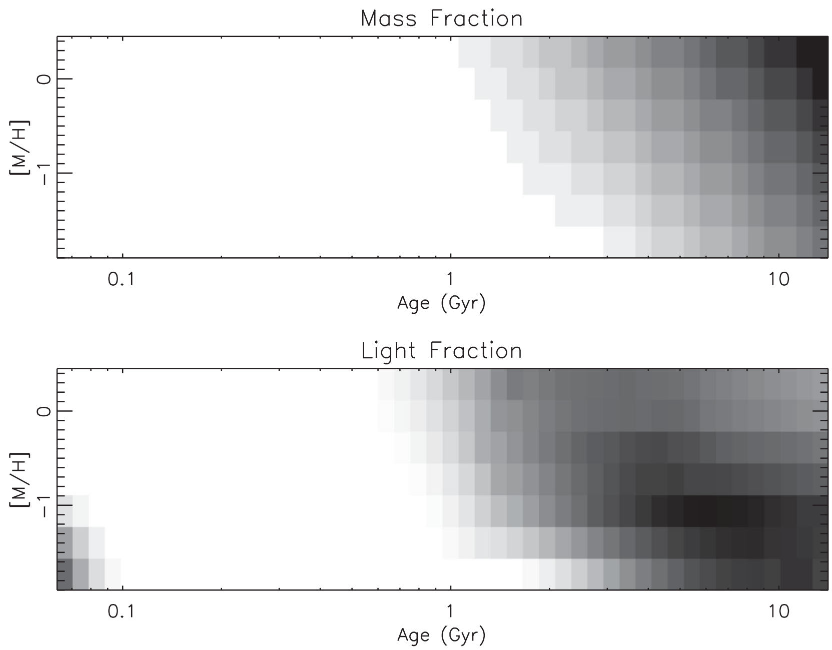

Figure 2. Relative mass and light fractions of different stellar populations in the host galaxy of XJ1231+1106 with respect to metallicity and age, with darker shading indicating a larger mass fraction in the best-fitting model. There seems to be a young (<90 Myr) population, based on the light fraction plot. The light was integrated over 3540 and 7410 Å.

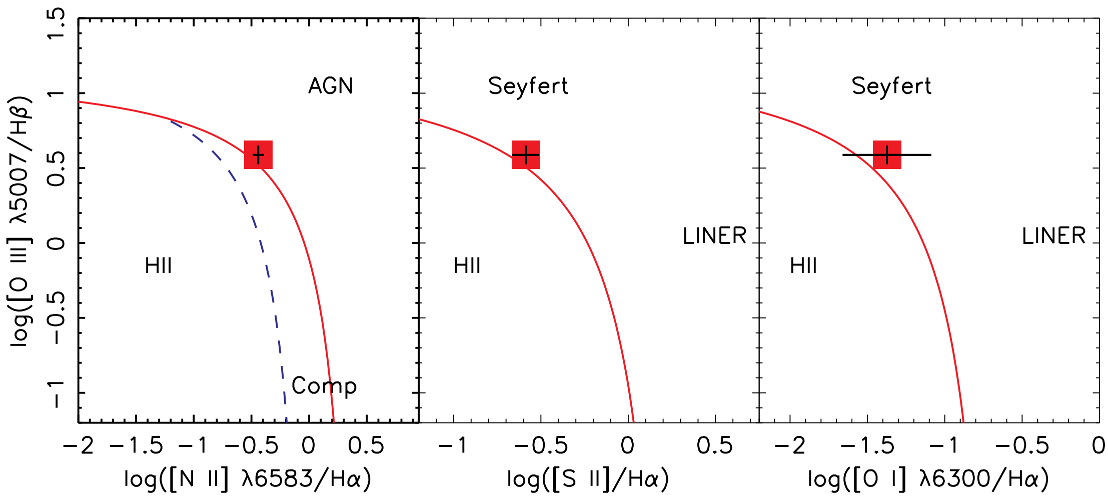

Figure 3. XJ1231+1106 on the BPT diagrams, indicating it as an AGN possibly with some star-forming activity. The dashed and solid lines are used to separate galaxies into H II-region-like, AGN and composite types (Kewley et al. 2006).

13). The *Chandra* spectrum seems very soft, with 11 counts below 0.7 keV (background is expected to be negligible). We rebinned the source spectrum to have at least one count per bin and carried out the fit with the multicolour disc (MCD) model and adopting the C statistic in XSPEC. The Galactic absorption was fixed at $N_{\mathrm{H}} = 2.3 \times 10^{20}$ cm^{-2} (Kalberla et al. 2005), and the intrinsic absorption was fixed at $N_{\mathrm{H,i}} = 6 \times 10^{19}$ cm^{-2} as obtained in Lin et al. (2013a). The fit is shown in Fig. 4 and given in Table 1. We inferred a source rest-frame disc temperature of $kT_{\mathrm{MCD}} = 0.09 \pm 0.02$ keV (90 per cent uncertainty). Given the low number of counts of the spectrum, we checked whether the fit was valid by simulating 1000 spectra of the same counts based on the best-fitting MCD model and then fitting with the same MCD model. We found that the best-fitting kT_{MCD} from the simulated spectra had the median and the scatter fully consistent with the best-fitting value and uncertainty of kT_{MCD} obtained above from the fit to the observed spectrum. Therefore, the source X-ray spectrum is not only fainter but also softer, at the confidence level of $\sim 5\sigma$, compared with the last *XMM–Newton* observation ($kT_{\mathrm{MCD}} = 0.18 \pm 0.01$ keV; Lin et al. 2013a). We note that the intrinsic absorption used to fit the *Chandra* spectrum was so low that assuming zero absorption would not change the inferred disc temperature, while assuming stronger absorption would infer a lower disc temperature. Therefore, our conclusion of the spectral softening is not subject to the intrinsic absorption assumed.

The source is also weakly detected in the combined *Swift* observations in 2013–2014. There are 28 counts within 0.3–10 keV, with 13 background counts expected (so 15 net source counts). The net source count rate is $2.9 \pm 1.0 \times 10^{-4}$ counts s^{-1} (1σ uncertainty),

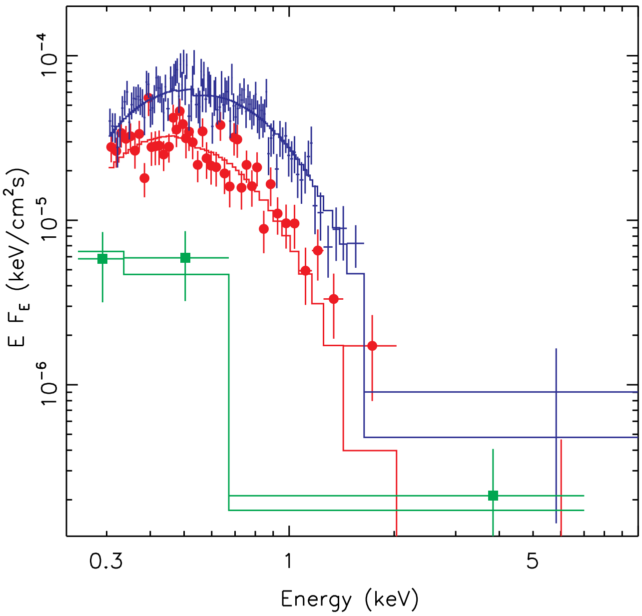

Figure 4. The example unfolded spectra of XJ1231+1106 fitted with the MCD model. From the top to the bottom are the second *XMM–Newton* observation (blue), the first *XMM–Newton* observation (2003 July 13, red filled circles) and the *Chandra* observation (green filled squares). For clarity, we show the pn data only for the *XMM–Newton* observations and have rebinned all spectra to be above 2σ per bin.

a factor of 11 lower than expected from the second *XMM–Newton* spectrum. The source spectrum was also soft, with 12.5 net source counts below 0.7 keV. We also carried out an MCD fit to this *Swift* spectrum and obtained $kT_{\rm MCD} = 0.15 \pm 0.05$ keV (Table 1). The large uncertainty makes it hard to conclude whether the source spectrum was softer than *XMM–Newton* observations, though it was significantly fainter.

The long-term luminosity evolution of the source based on the MCD fits is shown in Fig. 5. The source could be in an X-ray outburst, with the peak X-ray luminosity of $\sim$4 $\times$ 10^{42} erg s^{-1}, reached in the second and third *XMM–Newton* observations. The X-ray luminosity had decreased to $\sim$3 $\times$ 10^{41} erg s^{-1} in the *Chandra* observation. The bolometric luminosity was $\sim$10^{43} erg s^{-1} in these observations and is fairly independent of the spectral model (an MCD or optically thick low-temperature corona). The bolometric luminosity had decreased to $\sim$2 $\times$ 10^{42} erg s^{-1} in the *Chandra* observation.

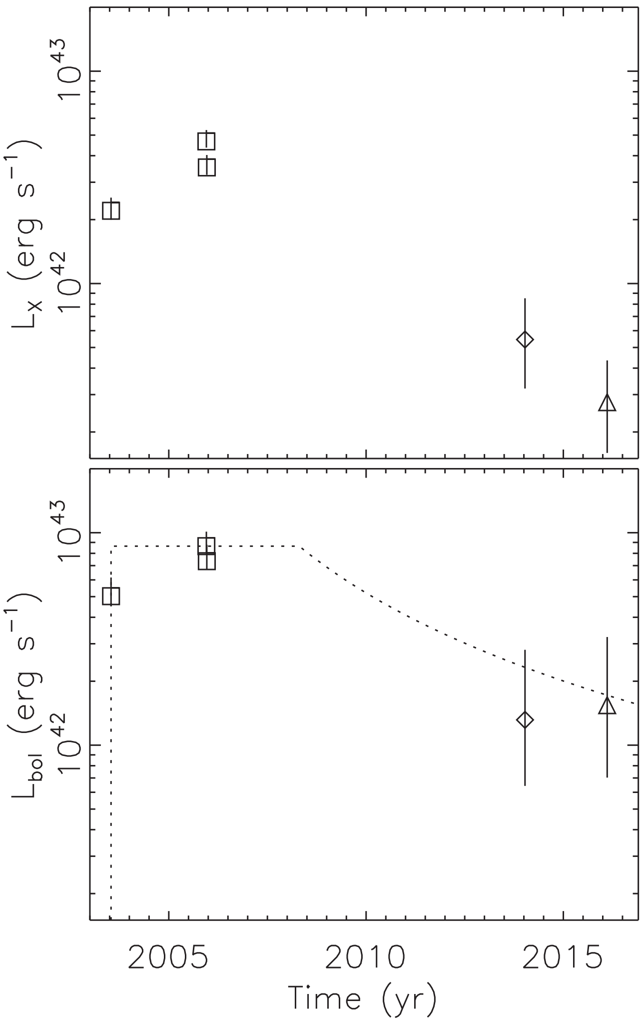

Figure 5. The long-term luminosity curve of XJ1231+1106 from the *XMM–Newton* (squares), *Swift* (diamond), *Chandra* (triangle) observations. The upper panel is for the 0.34–11 keV (source rest frame) unabsorbed luminosity, and the bottom panel is for the bolometric luminosity based on the MCD model. The dashed line plots a TDE model of prompt accretion (see Section 4 for more details).

4 DISCUSSION AND CONCLUSIONS

4.1 The AGN explanation

The main result of our follow-up observation of XJ1231+1106 is the detection of the significant drop and softening of its X-ray emission, suggesting that the source is probably in the decay of an X-ray outburst that has last for >13 yr. Because the narrow emission lines in the host galaxy spectrum signal the presence of a low-luminosity type-2 AGN, in principle, we cannot completely rule out that the X-ray outburst is purely due to AGN activity. However, pure thermal X-ray spectra are atypical for AGNs (e.g. Lin et al. 2012). The large variability of the source is uncommon for AGNs too (only 1.5 per cent of AGNs vary in X-rays by a factor of >10; Lin et al. 2012).

One possible explanation for XJ1231+1106 is an AGN flare caused by a disc instability, as proposed for NGC 3599 (Saxton et al. 2015) and IC 3599 (Grupe et al. 2015). The disc instability can cause large variability on time-scales of years for AGNs. However, we note that this mechanism is still poorly understood and that the observational evidence is still vague. For NGC 3599 and IC 3599, alternative explanations, especially TDEs, are still possible (Campana et al. 2015; Saxton et al. 2015).

Another possible explanation for the X-ray outburst of XJ1231+1106 is an AGN just entering a luminous thermal state, a common spectral state for BH X-ray binaries, in which the X-ray spectra were dominated by emission from a standard thermal thin disc. This explanation was proposed to explain the supersoft semipersistent X-ray outburst of GSN 069 (Miniutti et al. 2013). However, such a state would last >10^4 yr in AGNs if the analogy between BH X-ray binary transients and AGN holds, and this is in conflict with our detection of the large variability of the source flux within 10 yr.

4.2 The TDE explanation

Pure thermal X-ray spectra are commonly observed in sources suspected to be TDEs. Therefore, Lin et al. (2013a) discussed XJ1231+1106 as a possible TDE. This is further supported by our new detection of the outburst-like large variability of the source. One main difference between XJ1231+1106 and other TDE candidates is its slow evolution. The X-ray flux of other TDE candidates typically decreased by an order of magnitude in one year right after they were discovered (e.g. Komossa et al. 2004; Maksym et al. 2013), while it took 10 yr for the X-ray flux of XJ1231+1106 to decrease by one order of magnitude. The first *XMM–Newton* observation was even fainter (by a factor of 2) than the other two *XMM–Newton* observations 2.4 yr later. The X-ray spectral softening observed in XJ1231+1106 with the decrease in the X-ray flux has been observed in some TDE candidates (Lin et al. 2011; Saxton et al. 2012), but not in all cases. In the well monitored TDE candidate ASASSN-14li, steady blackbody temperatures in the X-ray spectra were observed despite the drop of the X-ray flux nearly by an order of magnitude (Miller et al. 2015). It is not clear what caused the above difference.

The slow decay and spectral softening of the X-ray emission make XJ1231+1106 somewhat similar to a long-lived TDE candidate 3XMM J150052.0+015452, which showed little decay of the X-ray flux over 10 yr after it went into an X-ray outburst and displayed dramatic spectral softening, from quasi-soft ($kT \sim 0.3$ keV) to supersoft ($kT \sim 0.13$ keV) X-ray spectra (Lin et al. 2017). One explanation for the slow decay of that source is the combination of slow circularization and super-Eddington accretion effects. Slow circularization occurs when the fallback of mass is faster than the accretion and have been predicted in many recent studies (Kochanek 1994; Guillochon & Ramirez-Ruiz 2015; Piran et al. 2015; Shiokawa et al. 2015; Hayasaki, Stone & Loeb 2016). Such events would evolve slower than those with prompt accretion. TDEs could have accretion rates above the Eddington limit initially. In this phase, significant super-Eddington effects of photon trapping and outflows in the inner disc region are expected (Ohsuga & Mineshige 2007; Krolik & Piran 2012; King & Muldrew 2016). These effects are stronger at higher accretion rates, resulting in a disc luminosity sustained at around the Eddington limit. Therefore, the decay of the flux would appear slow in the super-Eddington accretion phase. The identification of a long super-Eddington accretion phase in 3XMM J150052.0+015452 was strongly supported by the generally quasi-soft X-ray spectra, whose characteristic temperatures are too high to be explained by the standard thermal thin disc below the Eddington limit, but are consistent with Comptonized emission from a low-temperature optical thick corona. Similar spectra are commonly seen in ultraluminous X-ray sources (Gladstone, Roberts & Done 2009; Lin et al. 2013b; Middleton et al. 2013), most of which are believed to be super-Eddington accreting stellar-mass BHs, except that 3XMM J150052.0+015452 had orders of magnitude higher luminosities.

XJ1231+1106 was most likely in the thermal state, instead of a super-Eddington accretion state, in the *Swift* and *Chandra* observations, given the much lower luminosity and softer spectra in these observations than in the *XMM–Newton* ones. The spectral state identification for the *XMM–Newton* observations is more subtle. Lin et al. (2013a) found that the *XMM–Newton* X-ray spectra can be described with either pure thermal disc emission (i.e. the standard thermal state) or optically thick low-temperature Comptonization (characteristic of a super-Eddington accretion state). The former model requires a sub-Eddington luminosity. Due to the relatively high disc temperatures, this model required the BH to have mass $\sim 10^5$ $M_\odot$ and some spin. If the source was instead in a super-Eddington accretion state in the *XMM–Newton* observations, the BH should have mass below $\sim 10^5$ $M_\odot$ (but above 10^4 $M_\odot$, so that it can be in the standard thermal state in the *Swift* and *Chandra* observations). In either case, the BH mass should be small, agreeing with the estimate by Ho et al. (2012) and a little lower than our estimate above based on the stellar mass (the difference is not significant due to large scatter of the relation used).

In Fig. 5, we plot a model of the luminosity evolution assuming a full disruption of a solar-type star by a BH of mass 10^5 $M_\odot$, with prompt accretion (i.e. the mass accretion rate is equal to the mass fallback rate). In this case, the rising time is expected to be $\lesssim$1 month (Ulmer 1999; Guillochon & Ramirez-Ruiz 2015). The first *XMM–Newton* observation should be in the rising phase because the source had a lower luminosity in this observation than in the two observations 2.4 yr later. The super-Eddington accretion phase can last for 4.8 yr (Ulmer 1999). Therefore, the source luminosity was assumed to be constant in the initial 4.8 yr, at the Eddington limit (Krolik & Piran 2012), which was adopted to be that seen in the second *XMM–Newton* observation. After the super-Eddington accretion phase, the luminosity followed the standard evolution of the mass accretion rate as $(t - t_d)^{-5/3}$ (Rees 1988; Phinney 1989), where t_d is the disruption time, assumed to be one month before the first *XMM–Newton* observation.

This simple model of a TDE of prompt accretion seems to describe the data well. However, it would be highly coincident that the first *XMM–Newton* observation caught the fast rise. Alternatively, it could be a TDE of slow circularization and thus of a relatively long rising phase (Guillochon & Ramirez-Ruiz 2015). Tidal stripping of an evolved star could also result in a relatively slow event (MacLeod, Guillochon & Ramirez-Ruiz 2012). However, TDEs of evolved stars should be very rare for a BH of mass 10^5 $M_\odot$, accounting for only ∼3 per cent of the total TDEs (Kochanek 2016). Besides, in such events, the partial disruption is more likely, resulting in low luminosities (MacLeod et al. 2013), while our source had peak luminosity around the Eddington limit.

As shown in the BPT diagrams, the narrow emission lines in the SDSS spectrum of GJ1231+1106 could in some part be due to persistent nuclear activity. Then we expect the presence of a hard X-ray component if it is a normal AGN. The strength of this hard X-ray component can be estimated based on its normal correlation with the [O III] λ5007 emission line (Lamastra et al. 2009). The [O III] λ5007 emission line absorbed luminosity is $8.7 \pm 0.4 \times 10^{39}$ erg s^{-1}. The observed Hα/Hβ ratio is 4.3 ± 0.6, and assuming an intrinsic value of the ratio to be 3.1 would imply an intrinsic reddening of $E(B-V)_i = 0.30 \pm 0.14$ mag (Galactic reddening $E(B-V)_G = 0.03$ mag, Schlegel et al. 1998). Correcting for this reddening, the [O III] λ5007 luminosity is $2.5 \pm 1.1 \times 10^{40}$ erg s^{-1}. Using the [O III] λ5007 and 2–10 keV luminosity relation in Lamastra et al. (2009), whose dispersion is 0.63 dex, we estimated the persistent 2–10 keV luminosity to be $3.1 \pm 2.4 \times 10^{41}$ erg s^{-1} (the 1σ uncertainty has included the dispersion of the relation used). Assuming an absorbed power-law of photon index 2.0 and Galactic absorption, we expect to collect 12 ± 9 counts in 2–7 keV and 45 ± 35 counts in 0.7–7 keV in the *Chandra* observation, but only 1.5 net counts were detected in 0.7–7 keV. However, given the large uncertainty of the above estimate and the possible contribution of star-forming activity to the narrow emission lines, we cannot completely rule out that a persistent weak hard X-ray component is present but is too weak to be detected. Alternatively, it could be possible that the TDE has destroyed the corona or jet that is responsible for hard X-ray emission.

ACKNOWLEDGEMENTS

We thank the anonymous referee for the helpful comments. DL is supported by the National Aeronautics and Space Administration through Chandra Award Number GO5-16114X issued by the Chandra X-ray Observatory Center, which is operated by the Smithsonian Astrophysical Observatory for and on behalf of the National Aeronautics Space Administration under contract NAS8-03060. The work of LCH was supported by National Key Program for Science and Technology Research and Development grant 2016YFA0400702. We thank the Swift PI Neil Gehrels for approving our ToO request to make several observations of 2XMM J123103.2+110648.

Funding for SDSS-III has been provided by the Alfred P. Sloan Foundation, the Participating Institutions, the National Science Foundation, and the US Department of Energy Office of Science. The SDSS-III web site is http://www.sdss3.org/. SDSS-III is managed by the Astrophysical Research Consortium for the Participating Institutions of the SDSS-III Collaboration including the University of Arizona, the Brazilian Participation Group, Brookhaven National Laboratory, Carnegie Mellon University, University of Florida, the French Participation Group, the German Participation Group, Harvard University, the Instituto de Astrofisica de Canarias, the Michigan State/Notre Dame/JINA Participation Group, Johns Hopkins University, Lawrence Berkeley National Laboratory, Max Planck Institute for Astrophysics, Max Planck Institute for Extraterrestrial Physics, New Mexico State University, New York University, Ohio State University, Pennsylvania State University, University of Portsmouth, Princeton University, the Spanish Participation Group, University of Tokyo, University of Utah, Vanderbilt University, University of Virginia, University of Washington, and Yale University.

REFERENCES

Baldwin J. A., Phillips M. M., Terlevich R., 1981, PASP, 93, 5
Bautz M. W. et al., 1998, in Hoover R. B., Walker A. B., eds, Proc. SPIE Conf. Ser. Vol. 3444 X-Ray Optics, Instruments and Missions. SPIE, Bellingham, p. 210
Burrows D. N. et al., 2005, Space Sci. Rev., 120, 165
Campana S., Mainetti D., Colpi M., Lodato G., D'Avanzo P., Evans P. A., Moretti A., 2015, A&A, 581, A17
Cappellari M., Emsellem E., 2004, PASP, 116, 138
Comastri A., Setti G., Zamorani G., Elvis M., Wilkes B. J., McDowell J. C., Giommi P., 1992, ApJ, 384, 62
Gehrels N. et al., 2004, ApJ, 611, 1005
Gierliński M., Done C., 2004, MNRAS, 349, L7
Gladstone J. C., Roberts T. P., Done C., 2009, MNRAS, 397, 1836
Grupe D., Beuermann K., Mannheim K., Bade N., Thomas H.-C., de Martino D., Schwope A., 1995, A&A, 299, L5
Grupe D., Komossa S., Saxton R., 2015, ApJ, 803, L28
Guillochon J., Ramirez-Ruiz E., 2015, ApJ, 809, 166
Hayasaki K., Stone N., Loeb A., 2016, MNRAS, 461, 3760
Ho L. C., Kim M., Terashima Y., 2012, ApJ, 759, L16
Kalberla P. M. W., Burton W. B., Hartmann D., Arnal E. M., Bajaja E., Morras R., Pöppel W. G. L., 2005, A&A, 440, 775
Kewley L. J., Groves B., Kauffmann G., Heckman T., 2006, MNRAS, 372, 961
King A., Muldrew S. I., 2016, MNRAS, 455, 1211
Kochanek C. S., 1994, ApJ, 422, 508
Kochanek C. S., 2016, MNRAS, 461, 371
Komossa S., 2012, in EPJ Web Conf., 39 2001
Komossa S., 2015, JHEA, 7, 148
Komossa S., Halpern J., Schartel N., Hasinger G., Santos-Lleo M., Predehl P., 2004, ApJ, 603, L17
Krolik J. H., Piran T., 2012, ApJ, 749, 92
Lamastra A., Bianchi S., Matt G., Perola G. C., Barcons X., Carrera F. J., 2009, A&A, 504, 73
Lin D., Carrasco E. R., Grupe D., Webb N. A., Barret D., Farrell S. A., 2011, ApJ, 738, 52
Lin D., Webb N. A., Barret D., 2012, ApJ, 756, 27
Lin D., Irwin J. A., Godet O., Webb N. A., Barret D., 2013a, ApJ, 776, L10
Lin D., Irwin J. A., Webb N. A., Barret D., Remillard R. A., 2013b, ApJ, 779, 149
Lin D., Webb N. A., Barret D., 2014, ApJ, 780, 39
Lin D. et al., 2017, Nat. Astron., 1, 0033
Ludwig R. R., Greene J. E., Barth A. J., Ho L. C., 2012, ApJ, 756, 51
MacLeod M., Guillochon J., Ramirez-Ruiz E., 2012, ApJ, 757, 134
MacLeod M., Ramirez-Ruiz E., Grady S., Guillochon J., 2013, ApJ, 777, 133
Maksym W. P., Ulmer M. P., Eracleous M. C., Guennou L., Ho L. C., 2013, MNRAS, 435, 1904
Middleton M. J. et al., 2013, Nature, 493, 187
Miller J. M. et al., 2015, Nature, 526, 542
Miniutti G., Saxton R. D., Rodríguez-Pascual P. M., Read A. M., Esquej P., Colless M., Dobbie P., Spolaor M., 2013, MNRAS, 433, 1764
Nandra K., Pounds K. A., 1994, MNRAS, 268, 405
Ohsuga K., Mineshige S., 2007, ApJ, 670, 1283
Phinney E. S., 1989, in Morris M., ed., Proc. IAU Symp. 136, The Center of the Galaxy. Kluwer, Dordrecht p. 543
Piran T., Svirski G., Krolik J., Cheng R. M., Shiokawa H., 2015, ApJ, 806, 164
Rees M. J., 1988, Nature, 333, 523
Reines A. E., Volonteri M., 2015, ApJ, 813, 82
Roming P. W. A. et al., 2005, Space Sci. Rev., 120, 95
Saxton R. D., Read A. M., Esquej P., Komossa S., Dougherty S., Rodriguez-Pascual P., Barrado D., 2012, A&A, 541, A106
Saxton R. D., Motta S. E., Komossa S., Read A. M., 2015, MNRAS, 454, 2798
Schlegel D. J., Finkbeiner D. P., Davis M., 1998, ApJ, 500, 525
Shiokawa H., Krolik J. H., Cheng R. M., Piran T., Noble S. C., 2015, ApJ, 804, 85
Terashima Y., Kamizasa N., Awaki H., Kubota A., Ueda Y., 2012, ApJ, 752, 154
Turner T. J., Pounds K. A., 1989, MNRAS, 240, 833
Ulmer A., 1999, ApJ, 514, 180
Vazdekis A., Sánchez-Blázquez P., Falcón-Barroso J., Cenarro A. J., Beasley M. A., Cardiel N., Gorgas J., Peletier R. F., 2010, MNRAS, 404, 1639
Veilleux S., Osterbrock D. E., 1987, ApJS, 63, 295
Voges W. et al., 1999, A&A, 349, 389
Wilkes B. J., Elvis M., 1987, ApJ, 323, 243

This paper has been typeset from a TEX/LATEX file prepared by the author.